ISLAMIC UNIVERSITY OF TECHNOLOGY, (IUT)

Controlling of Grid Connected Solid Oxide Fuel Cell Power Generation

By

Md. Ahsanul Habib (092443)

Md. Mahmudur Rahman Khan (092444)

Md. Sabbir Hossain Chowdhury (092467)

Supervised By

Ashik Ahmed

Assistant Professor,

Department of Electrical and Electronic Engineering

Islamic University of Technology (IUT)

A Subsidiary Organization of OIC.

Dhaka, Bangladesh.

Acknowledgements

First of all, we would like to express our deep and sincere gratitude to our respected supervisor **Ashik Ahmed**, assistant professor in Electrical and Electronic Engineering department of Islamic University of Technology (IUT), Dhaka, Bangladesh, for his kind guidance and supervision on this thesis work. His regular and well supervision, kind helps, patience made this thesis gain its goal.

Second, we would like to express our deepest cordial thanks to all of our teachers for their supports and helpful attitude without which this thesis work might not bear fruit.

Finally, we would like to thank our parents who gave us hopes and inspirations.

Abstract

It is foreseen that Fuel Cells (FC) might be used jointly with conventional generation system to contribute to the grid in near future. The increase of electricity consumption, rapid decaying of fossil fuel, efficiency and cost effectiveness of FC are the crucial factors functioning behind this anticipation. But this practice can affect the stability conditions of the total power system. Hence, it is of the essence to contemplate the power system stability condition when SOFC (Solid Oxide Fuel Cell) power plant appended to it.

In this thesis the dynamic model of grid connected SOFC power plant which is additionally operating with conventional fossil-fuel generation system is simulated and the stability conditions are observed carefully. Later on, some FC controllers are utilized to regain the power system stability after occurring disturbances.

Keywords

SOFC, Power System Stability, FC controller, Dynamic Model, Non-linear model

Contents

Chapter 1
Introduction

1.1. Introduction

Fuel Cells (FC) are becoming a promising alternative to conventional fossil-fuel based electrical power plant because of their being highly efficient (33-60%) with zero to low emission, modular, environmentally friendly energy conversion devices [1], [2]. FC is categorized into various kinds among which the Solid Oxide Fuel Cell (SOFC) is considered to be the most attractive FC technology suitable for grid connected power generation [3]. As the FC technology is advancing rapidly it is anticipated that the grid connected large scale FC generation will not only affect the distribution network but also the transmission system and the other generation systems [2]. Hence, the FC connected power system security and stability should be analyzed with paramount importance [4]-[8].

The objective of this paper is to investigate the power system stability when FC is operating and contributing to the grid together with conventional power generator and also designing FC controllers to ensure the power system stability. The power system stability is rifely affected by the conventional generation system. This paper investigates that when the FC is appended to the system, where conventional generation system is already operating, how and why the small signal stability of the power system is affected. At the same time this paper includes the design of FC controller to make the system adhere to stability.

As an initiative, this paper first considers a single machine infinite-bus system and investigates the stability conditions with and without disturbance. Afterwards, an SOFC is considered to be connected to the infinite-bus system along with the single machine and the power system stability is examined once more. The capacity of the SOFC power plant is considered to be comparable to that of synchronous generator. To make this consideration more convenient it is assumed that the SOFC plant represents the integrated effect of many FC generation units.

1.2 Power system stability

Power system stability may be defined as that property of the system which enables the synchronous machines of the system to respond to a disturbance from a normal operating condition so as to return to a condition where their operation is again normal.

The power system stability is divided into two classes:

1. Steady state/small signal stability

   Small disturbances are continually occurring in a power system (variations in loadings, changes in turbine speed etc.) which are small enough not to cause the system to lose synchronism but do excite the system into the state of natural oscillations.

   Steady state stability is a particular steady state operating condition of the system which follows any small disturbance, it reaches a steady state operating condition which is identical or close to the pre-disturbance operating condition. Steady state stability is a function of only the operating condition. Historically steady-state instability has been associated with angle instability and slow loss of synchronism among generators.

2. Dynamic/Transient stability

   A system is said to be dynamically stable if the oscillations do not acquire more than certain amplitude and die out quickly (i.e. the system is well damped). In a dynamically unstable system, the oscillation amplitude is large and these persist for a long time (i.e. the system is underdamped). This kind of instability behavior constitutes a serious threat to system security and creates very difficult operating conditions.

   Transient stability is a function of both the operating condition and the disturbance(s).

1.3. Fuel cell :

A fuel cell is a device that converts the chemical energy from a fuel into electricity through a chemical reaction with oxygen or another oxidizing agent. Hydrogen is the most common fuel, but hydrocarbons such as natural gas and alcohols like methanol are sometimes used. Fuel cells are different from batteries in that they require a constant source of fuel and oxygen to run, but they can produce electricity continually for as long as these inputs are supplied.

In 1838, German Physicist Christian Friedrich Schönbein invented the first crude fuel cell. A year later Welsh Physicist William Grove developed his first crude fuel cells in 1839. The first commercial use of fuel cells was in NASA space programs to generate power for probes, satellites and space capsules. Since then, fuel cells have been used in many other applications. Fuel cells are used for primary and backup power for commercial, industrial and residential buildings and in remote or inaccessible areas. They are used to power fuel cell vehicles, including automobiles, buses, forklifts, airplanes, boats, motorcycles and submarines.

1.3.1. Working principle of fuel cell:

There are many types of fuel cells, but they all consist of an anode (negative side), a cathode (positive side) and an electrolyte that allows charges to move between the two sides of the fuel cell. Electrons are drawn from the anode to the cathode through an external circuit, producing direct current electricity. Individual fuel cells produce relatively small electrical potentials, about 0.7 volts, so cells are "stacked", or placed in series, to increase the voltage and meet an application's requirements. In addition to electricity, fuel cells produce water, heat and, depending on the fuel source, very small amounts of nitrogen dioxide and other emissions. The energy efficiency of a fuel cell is generally between 40–60%, or up to 85% efficient if waste heat is captured for use.

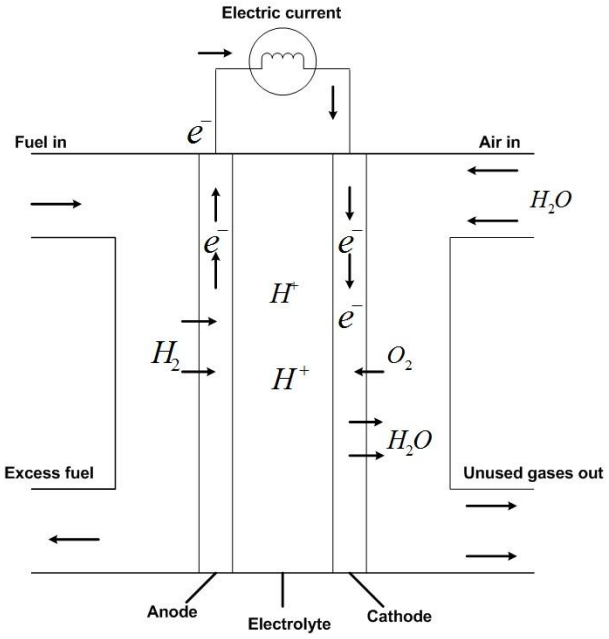

Fig.1 Working principle of fuel cell

1.3.2. Types of fuel cell

Fuel cells are divided according to their structure and electrolytic materials. Some of the useful types are:

1. Direct carbon fuel cell
2. Magnesium-Air Fuel Cell
3. Microbial fuel cell
4. Direct formic acid fuel cell (DFAFC)
5. Regenerative fuel cell
6. Direct methanol fuel cell
7. Reformed methanol fuel cell
8. Direct-ethanol fuel cell
9. Proton exchange membrane fuel cell
10. Tubular solid oxide fuel cell (TSOFC)
11. Planar Solid oxide fuel cell
12. Phosphoric acid fuel cell
13. Molten carbonate fuel cell
14. RFC - Redox

15. Protonic ceramic fuel cell
16. Metal hydride fuel cell
17. Electro-galvanic fuel cell
18. Zinc-air battery
19. Direct borohydride fuel cell
20. Alkaline fuel cell
21. Enzymatic Biofuel Cells
22. Upflow microbial fuel cell (UMFC)

1.3.3. Solid oxide fuel cell (SOFC)

Solid oxide fuel cells (SOFCs) use a solid material, most commonly a ceramic material called yttria-stabilized zirconia (YSZ), as the electrolyte. Because SOFCs are made entirely of solid materials, they are not limited to the flat plane configuration of other types of fuel cells and are often designed as rolled tubes. They require high operating temperatures (800 to 1000 °C) and can be run on a variety of fuels including natural gas.

SOFCs are unique in that negatively charged oxygen ions travel from the cathode (negative side of the fuel cell) to the anode (positive side of the fuel cell) instead of positively charged hydrogen ions travelling from the anode to the cathode, as is the case in all other types of fuel cells. Oxygen gas is fed through the cathode, where it reacts with electrons to create oxygen ions. The oxygen ions then travel through the electrolyte to react with hydrogen gas at the anode. The reaction at the anode produces electricity and water as by-products.

Carbon dioxide may also be a by-product depending on the fuel, but the carbon emissions from an SOFC system are less than those from a fossil fuel combustion plant. The chemical reactions for the SOFC system can be expressed as follows:

Anode Reaction: $2H_2 + 2O^{2-} \rightarrow 2H_2O + 4e^-$
Cathode Reaction: $O_2 + 4e^- \rightarrow 2O^{2-}$
Overall Cell Reaction: $2H_2 + O_2 \rightarrow 2H_2O$

SOFC systems can run on fuels other than pure hydrogen gas. However, since hydrogen is necessary for the reactions listed above, the fuel selected must contain hydrogen atoms. For the fuel cell to operate, the fuel must be converted into pure hydrogen gas. SOFCs are capable of internally reforming light hydrocarbons such as methane (natural gas), propane and butane. These fuel cells are at an early stage of development.

Challenges exist in SOFC systems due to their high operating temperatures. One such challenge is the potential for carbon dust to build up on the anode, which slows down the internal reforming process. Research to address this "carbon coking" issue at the University of Pennsylvania has shown that the use of copper-based cermet (heat-resistant materials made of ceramic and metal) can reduce coking and the loss of performance. Another disadvantage of SOFC systems is slow start-up time, making SOFCs less useful for mobile applications. Despite these disadvantages, a high operating temperature provides an advantage by removing the need for a precious metal catalyst like platinum, thereby reducing cost. Additionally, waste heat from SOFC systems may be captured and reused, increasing the theoretical overall efficiency to as high as 80%–85%.

The high operating temperature is largely due to the physical properties of the YSZ electrolyte. As temperature decreases, so does the ionic conductivity of YSZ. Therefore, to obtain optimum performance of the fuel cell, a high operating temperature is required. According to their website, Ceres Power, a UK SOFC fuel cell manufacturer, has developed a method of reducing the operating temperature of their SOFC system to 500–600 degrees Celsius. They replaced the commonly used YSZ electrolyte with a CGO (cerium gadolinium oxide) electrolyte. The lower operating temperature allows them to use stainless steel instead of ceramic as the cell substrate, which reduces cost and start-up time of the system.

1.4 Method of simulation

In this paper the non-linear model of single machine infinite-bus system and the non-linear model of SOFC power plant connected to infinite bus together with conventional generation are developed through equations. These models are then simulated using the software MATLAB.

After that, the stability conditions of the models are observed and finally, three FC controllers are designed through manual tuning of controller gain to keep the system stable.

1.5 Structure of the thesis

This paper is divided into 5 chapters. The main objective and goal is highlighted in the abstract part of the thesis. The thesis starts with the analysis of the non-linear model of single machine infinite-bus system and ends with the fuel cell controller designing and result issuing.

In chapter 1, a brief discussion of our total thesis work is given in the introduction. Then in chapter 2, the non-linear model of single machine infinite –bus system is analyzed. Afterwards, the non-linear model of SOFC power plant operating side by side to a conventional generator in a power system is investigated. The results and the graphs of these simulations are emerged in chapter 4. The thesis ends with a conclusion in chapter 5 in which a brief of our future plan about SOFC is anticipated.

Chapter 2
Modeling of a Synchronous Generator

2.1 Modeling of a Synchronous Generator Connected to Infinite Bus:

A single machine Connected to an infinite bus (SMIB) is although not so realistic for simplicity that can be considered. The system considered is in fig. q . This shows the external network with two ports. One port is connected to generator terminals while the second port is connected to a voltage source $E_b\angle 0$.Both the magnitude E_b and the phase angle of the voltage source are assumed to be constants. Also there is no loss of generality in assuming the phase angle of bus voltage as zero.

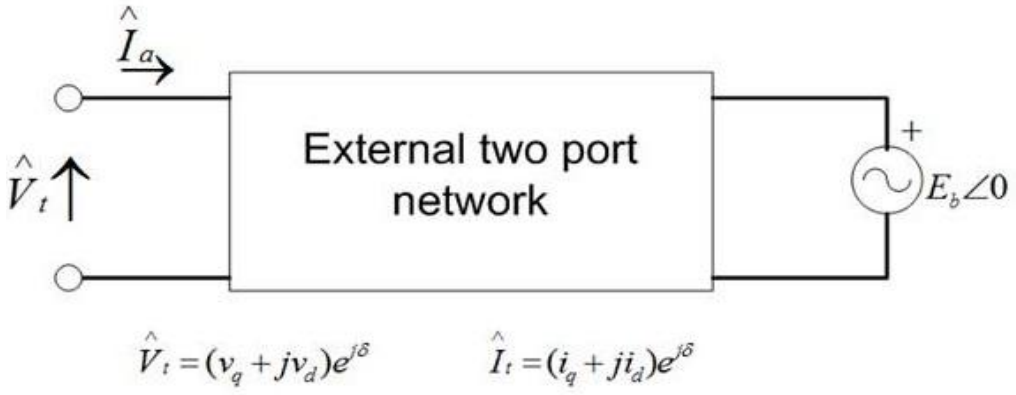

Fig.2.1 External two port network

The machine equations are

$$\frac{d\delta}{dt} = \omega_B(S_m - S_{m0}) \tag{2.1}$$

$$\frac{dS_m}{dt} = \frac{1}{2H}[-D(S_m - S_{m0}) + T_m - T_e] \tag{2.2}$$

$$\frac{dE'_q}{dt} = \frac{1}{T'_{d0}}[-E'_q + (x_d - x'_d)i_d + E_{fd}] \tag{2.3}$$

$$\frac{dE'_d}{dt} = \frac{1}{T'_{q0}}[-E'_d - (x_q - x'_q)i_q] \tag{2.4}$$

2.2 Initial Conditions

Initial conditions are given below,

$$\hat{I}_{ao} = I_{ao}\angle\phi_0 = \frac{P_t - jQ_t}{V_{t0}\angle -\theta_0} \tag{2.5}$$

$$E_{q0}\angle\delta_0 = V_{t0}\angle\theta_0 + (R_a + jx_q)I_{a0}\angle\phi_0 \tag{2.6}$$

$$i_{d0} = I_{a0}\sin(\delta_0 - \phi_0) \tag{2.7}$$

$$i_{q0} = I_{a0}\cos(\delta_0 - \phi_0) \tag{2.8}$$

$$v_{d0} = -v_{t0}\sin(\delta_0 - \phi_0) \tag{2.9}$$

$$E_{fd0} = E_{q0} + (x_d - x_q)i_{d0} \tag{2.10}$$

$$E'_{q0} = E_{q0} - (x_d - x'_d)i_{d0} \tag{2.11}$$

$$E'_{d0} = (x_q - x'_q)i_{q0} \tag{2.12}$$

$$T_{e0} = E'_{q0}i_{q0} + E'_{d0}i_{do} + (x'_d - x'_q)i_{d0}i_{qo} = T_{m0} \tag{2.13}$$

2.3 Simulation for a System Diagram

We added disturbance to simulate the real time disturbances occur in the practical network. Assume E_b =1.0.We got the following curves for different cases. Different initial values for different cases are given below as a table,

Variable	Case(1)	Case(2)	Case(3)	Case(4)
δ	44.1	69.73^o	30.27^o	71.28^o
E'_q	1.111	0.6814	0.9312	0.3893
E'_d	-0.4568	-0.6126	-0.3273	-0.6245
i_d	-0.9332	-0.7813	-0.1536	-0.1535
i_q	0.3597	0.4835	0.2577	0.4838
E_{fd}	2.6787	2.0094	1.1923	0.6503
V_t	1.0928	0.9804	1.0022	0.9232

Case 1: Pt=0.9 and Qt=0.9

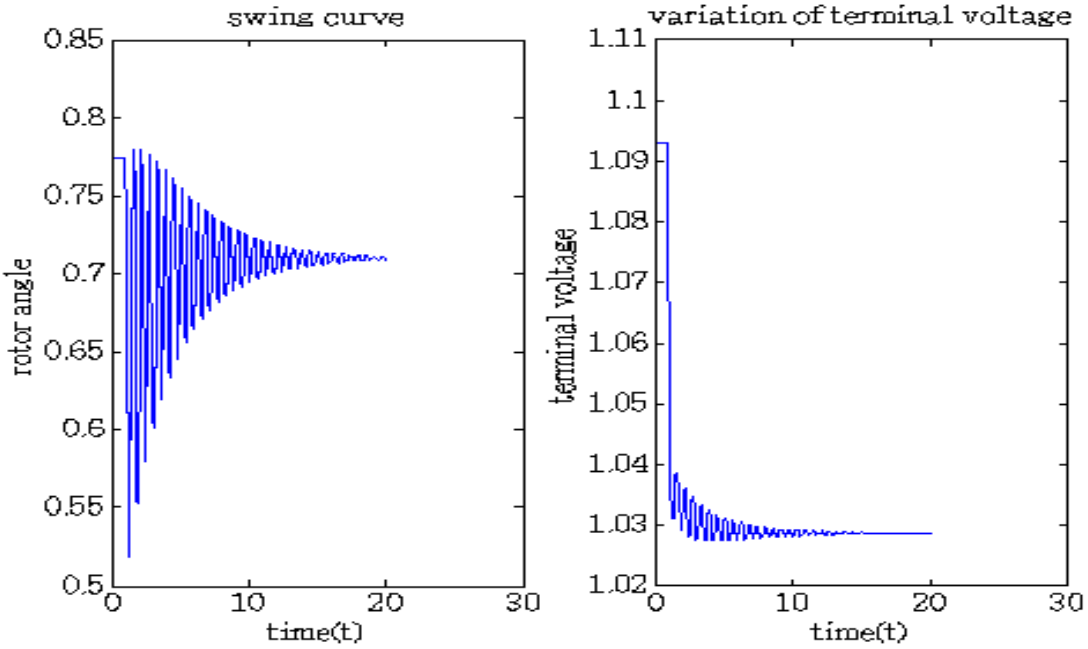

Fig. 2.2 Swing curve and Terminal voltage curve (Case 1)

Case 2: Pt=0.9 and Qt=-0.02

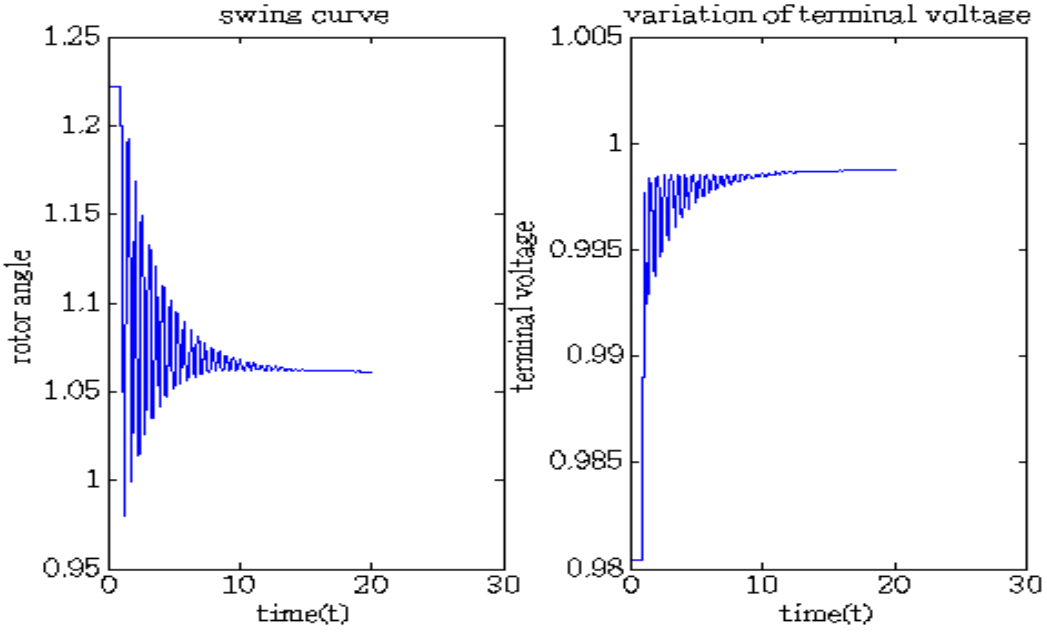

Fig. 2.3 Swing curve and Terminal voltage curve (case 2)

Case 3: Pt=0.3 and Qt=0.02

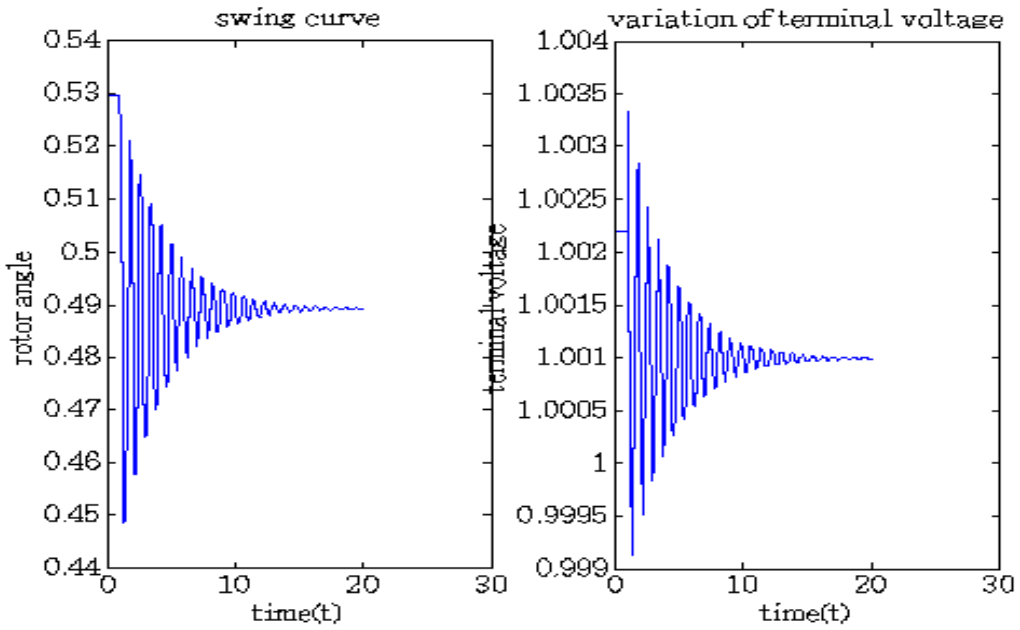

Fig. 2.4 Swing curve and Terminal voltage curve (case 3)

Case 4: Pt=0.3 and Qt=-0.36

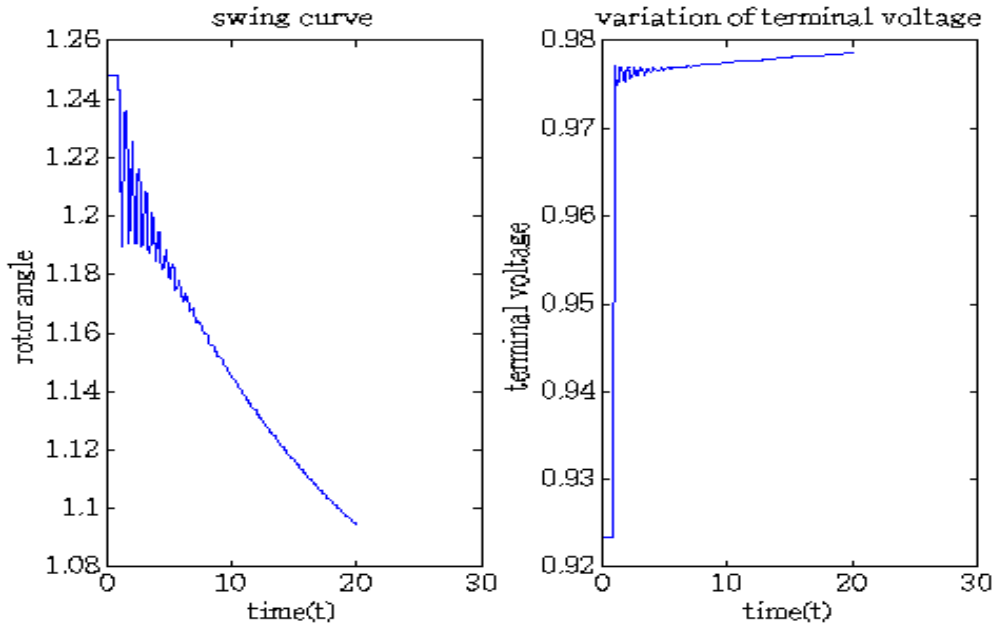

Fig. 2.5 Swing curve and Terminal voltage curve (case 4)

2.4 Analysis of Single Machine System

With classical model of the synchronous machine, the steady state instability at the limiting power is characterized by a slow monotonic increase (or decrease) in the rotor angle, resulting in loss of synchronism. With the advent of automatic voltage regulator (AVR) it was felt that the steady state stability limit can be enhanced as the AVR acts to overcome the armature reaction. A simplified representation of the effect of AVR is the reduction of the generator reactance from xd to a much smaller value. It is to be noted that without AVRs modern turbo-generators cannot operate at full rated power. Also, the transient stability is improved by fast acting exciters with high gain.

2.4.1. Small Signal Stability with block diagram representation

Consider a single machine system shown in Fig. 2.6. For simplicity we will assume a synchronous machine represented by model 1.0 neglecting damper windings both in d and q axes. Also the armature resistance of the machine is neglected and the excitation system represented by a single time-constant system shown in Fig. 2.7.

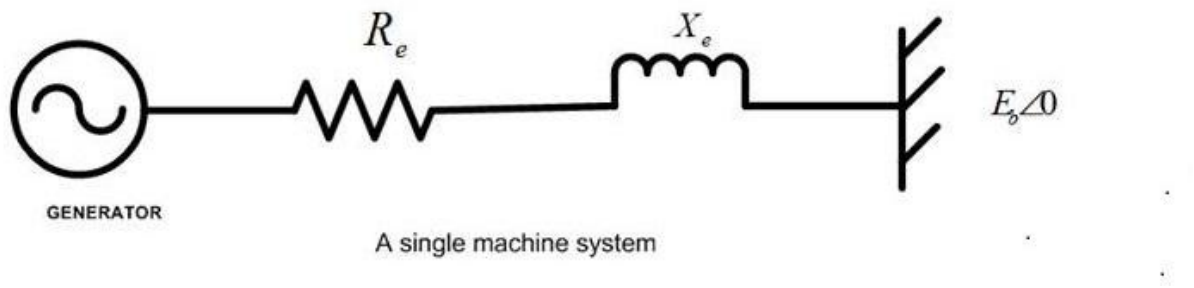

Fig. 2.6 A Single Machine System

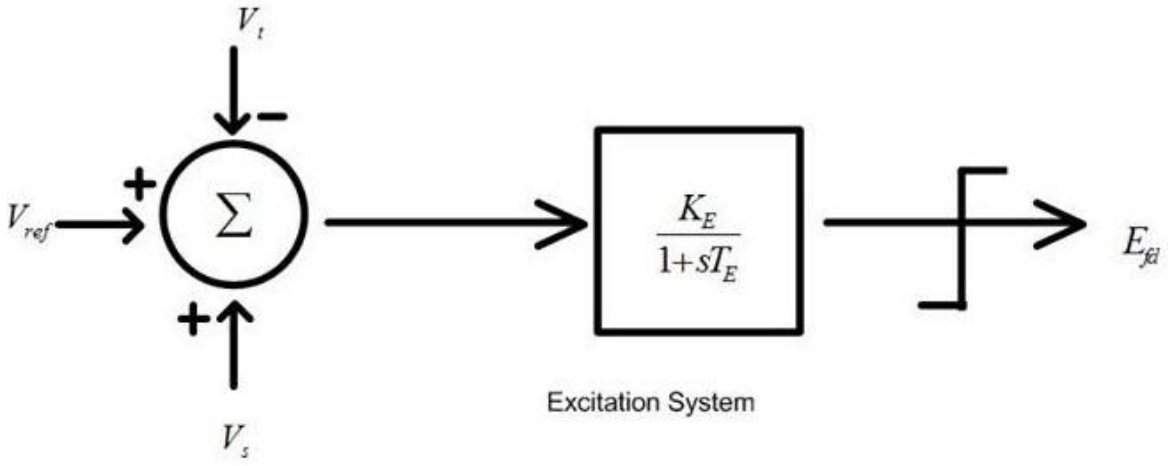

Fig 2.7 Excitation system

The algebraic equations of the stator are

$$E'_q + x'_d i_d = v_q \tag{2.14}$$

$$-x_q i_q = v_d \tag{2.15}$$

The complex terminal voltage can be expressed as

$$(v_q + jv_d) = (i_q + ji_d)(R_e + jx_e) + E_b e^{-j\delta} \tag{2.16}$$

Separating real and imaginary parts Eq. (2.16) can be expressed as

$$v_q = R_e i_q - x_e i_d + E_b \cos\delta \tag{2.17}$$

$$v_d = R_e i_d + x_e i_q - E_b \sin\delta \tag{2.18}$$

Substituting Eqs. (2.17) and (2.18) in Eq. (2.14) and (2.15), we get,

$$\begin{pmatrix} (x'_d + x_e) & -R_e \\ -R_e & -(x_q + x_e) \end{pmatrix} \begin{pmatrix} i_d \\ i_q \end{pmatrix} = \begin{pmatrix} E_b \cos\delta - E'_q \\ -E_b \sin\delta \end{pmatrix} \tag{2.19}$$

After linearizing we get,

$$\Delta i_d = C_1 \Delta\delta + C_2 \Delta E'_q \tag{2.20}$$

$$\Delta i_q = C_3 \Delta\delta + C_4 \Delta E'_q \tag{2.21}$$

Where

$$C_1 = \frac{1}{A}[R_e E_b \cos\delta_0 - (x_q + x_e) E_b \sin\delta_0]$$

$$C_2 = -\frac{1}{A}(x_q + x_e)$$

$$C_3 = \frac{1}{A}[(x'_d + x_e) E_b \cos\delta_0 + R_e E_b \sin\delta_0]$$

$$C_4 = \frac{R_e}{A}$$

Linearizing Eq. (2.14) and (2.15) and substituting from Eq. (2.20) and (2.21), we get,

$$\Delta v_d = x'_d C_1 \Delta\delta + (1 + x'_d C_2)\Delta E'_q \quad (2.22)$$

$$\Delta v_q = -x_q C_3 \Delta\delta - x_q C_4 \Delta E'_q \quad (2.23)$$

2.4.2. Rotor Mechanical Equation and Torque Angle Loop

The rotor angle mechanical equations are

$$\frac{d\delta}{dt} = \omega_B (S_m - S_{m0}) \quad (2.24)$$

$$2H\frac{dS_m}{dt} = -DS_m + T_m - T_e \quad (2.25)$$

$$T_e = E'_q i_q - (x_q - x'_d) i_d i_q \quad (2.26)$$

After linearizing Eq. (2.26), we get,

$$\Delta T_e = K_1 \Delta\delta + K_2 \Delta E'_q \quad (2.27)$$

Where

$$K_1 = E_{q0} C_3 - (x_q - x'_d) i_{q0} C_1 \quad (2.28)$$

$$K_2 = E_{q0} C_4 + i_{q0} - (x_q - x'_d) i_{q0} C_2 \quad (2.29)$$

$$E_{q0} = E'_{q0} - (x_q - x'_d) i_{d0} \quad (2.30)$$

2.4.3. Representation of Flux Decay

The equation of field winding can be expressed as

$$T'_{d0}\frac{dE'_q}{dt} = E_{fd} - E'_q + (x_d - x'_d)i_d \tag{2.31}$$

Linearizing the equation we get,

$$T'_{d0}\frac{d\Delta E'_q}{dt} = \Delta E_{fd} - \Delta E'_q + (x_d - x'_d)(C_1\Delta\delta + C_2\Delta E'_q) \tag{2.32}$$

Taking laplace transform we get,

$$(1+sT'_{d0}K_3)\Delta E'_q = K_3\Delta E_{fd} - K_3K_4\Delta\delta \tag{2.33}$$

where

$$K_3 = \frac{1}{[1-(x_d - x'_d)C_2]} \tag{2.34}$$

$$K_4 = -(x_d - x'_d)C_1 \tag{2.35}$$

2.4.4 Representation of Excitation system

The presentation of terminal voltage V_t can be expressed as,

$$\Delta V_t = \frac{v_{do}}{V_{t0}}\Delta v_d + \frac{v_{qo}}{V_{t0}}\Delta v_q \tag{2.36}$$

In general form

$$\Delta V_t = K_5\Delta\delta + K_6\Delta E'_q \tag{2.37}$$

Where

$$K_5 = (\frac{v_{d0}}{V_{t0}})x_qC_3 + (\frac{v_{q0}}{V_{t0}})x'_dC_1 \tag{2.38}$$

$$K_6 = -(\frac{v_{d0}}{V_{t0}})x_qC_4 + (\frac{v_{q0}}{V_{t0}})(1-x'_dC_2) \tag{2.39}$$

2.4.5. Computation Heffron-Philips Constants for Lossless Network

For R_e=0, the expressions for the constants K_1 to K_6 are simplified. As the armature resistance is already neglected, this refers to a lossless network on the stator side. The expressions are given below;

$$K_1 = \frac{E_b E_{q0} \cos\delta_0}{(x_e + x_q)} + \frac{(x_q - x'_d)}{(x_e + x'_d)} E_b i_{q0} \sin\delta_0 \tag{2.40}$$

$$K_2 = \frac{(x_e - x_q)}{(x_e + x'_d)} i_{q0} = \frac{E_b \sin\delta_0}{(x_e + x'_d)} \tag{2.41}$$

$$K_3 = \frac{(x_e - x'_d)}{(x_e + x_d)} \tag{2.42}$$

$$K_4 = \frac{(x_d - x'_d)}{(x_e + x'_d)} E_b \sin\delta_0 \tag{2.43}$$

$$K_5 = \frac{-x_q v_{d0} E_b \cos\delta_0}{(x_e + x_q) V_{t0}} - \frac{x'_d v_{q0} E_b \sin\delta_0}{(x_e + x'_d) V_{t0}} \tag{2.44}$$

$$K_6 = \frac{x_e}{(x_e + x'_d)} . (\frac{v_{q0}}{V_{t0}}) \tag{2.45}$$

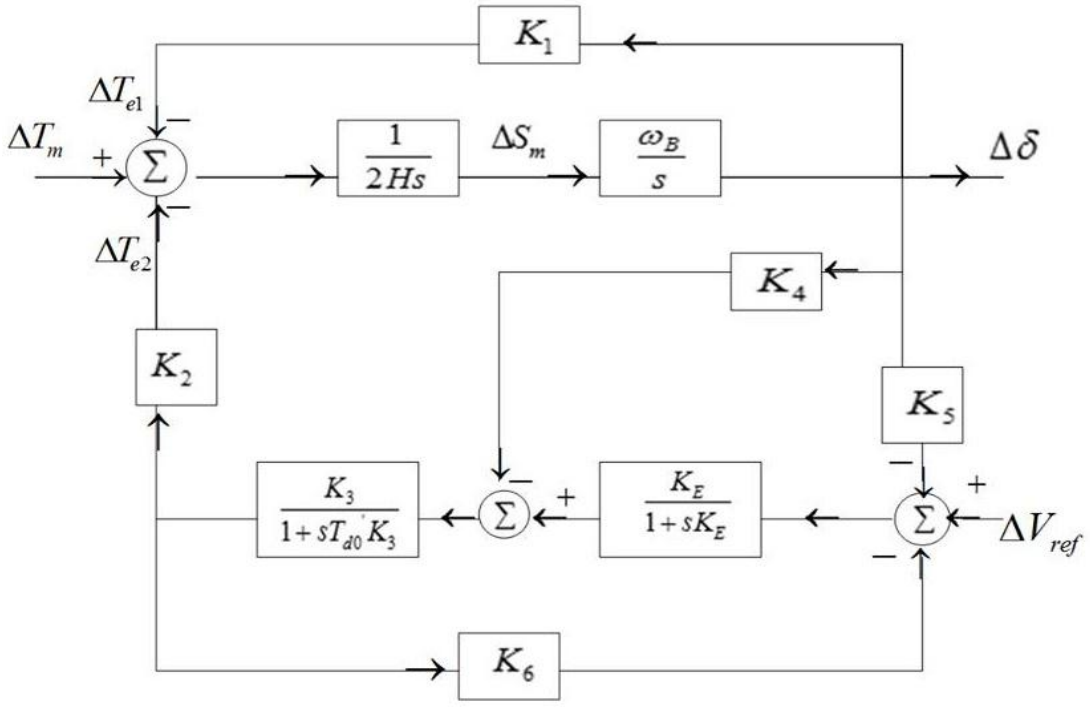

Fig.2.8 Overall block diagram

2.4.6 Simplified Model with State Equation

It is possible to express the system equation in the state space form. From the block diagram, Fig.2.8 The following system equations can be derived

$$\dot{x} = [A]x + [B](\Delta V_{ref} + \Delta V_s) \tag{2.46}$$

where

$$x^t = \begin{bmatrix} \Delta\delta & \Delta S_m & \Delta E'_q & \Delta E_{fd} \end{bmatrix}$$

$$[A] = \begin{pmatrix} 0 & \omega_B & 0 & 0 \\ -\frac{K_1}{2H} & -\frac{D}{2H} & -\frac{K_2}{2H} & 0 \\ -\frac{K_4}{T'_{d0}} & 0 & -\frac{1}{T'_{d0}K_3} & \frac{1}{T'_{d0}} \\ -\frac{K_E K_5}{T_E} & 0 & -\frac{K_E K_6}{T_E} & -\frac{1}{T_E} \end{pmatrix}$$

$$[B]^t = [0 \quad 0 \quad 0 \quad \frac{K_E}{T_E}]$$

The damping term D, is included in the swing equation. The eigenvalue of the matrix should lie in LHP in the ‘s’ plane for the system to be stable. The effect of various parameters (KE and TE) can be exclaimed from eigenvalue analysis. It is to be noted that the elements of matrix [A] are dependent on the operating condition.

Chapter 3
Controlling of Grid connected SOFC

3.1 Machine model of Conventional Single machine power system

The configuration of SOFC power plant connected to the grid is shown in Fig. 3.1. A single-machine infinite bus power system can be modeled by a system of nonlinear equations of the form

$$\dot{X} = f(X, \bar{I}_{ts}) \tag{3.1}$$

where, X is the vector of state variables and $\bar{I}_{ts}$ is the vector of input variables. In d-q coordinate of the single machine I can be stated by its d and q parts i_{tsd} and i_{tsq} respectively.

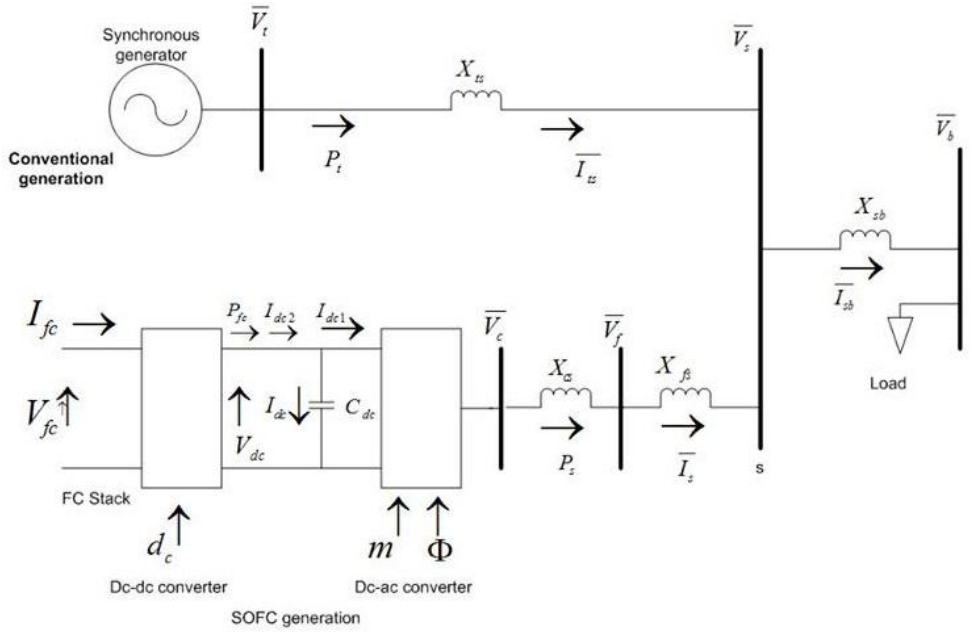

Fig.3.1 Configuration of a SOFC power plant connected to a single machine infinite bus power system [2]

Machine model equations are,

$$\dot{\delta} = \omega_o(\omega - 1)$$

$$\dot{\omega} = \frac{1}{M}[P_m - P_t - D(\omega - 1)]$$

$$\dot{E}'_q = \frac{1}{T'_{d0}}(-E'_q + E'_{fd}) \tag{3.2}$$

$$\dot{E}'_{fd} = -\frac{1}{T_A}E'_{fd} + \frac{K_A}{T_A}(V_{ref} - V_t)$$

with $X = [\delta \quad \omega \quad E'_q \quad E'_{fd}]^T$

where

$$P_t = E'_q i_{tsq} + (x_q - x'_d) i_{tsd} i_{tsq}$$

$$E_q = E'_q + (x_d - x'_d) i_{tsd} \tag{3.3}$$

$$V_t = \sqrt{v_{td}^2 + v_{tq}^2} = \sqrt{(x_q i_{tsq})^2 + (E'_q - x'_d i_{tsd})^2}$$

3.2. Modeling of Solid Oxide Fuel Cell (SOFC) Power Plant into a Power

FC electrical dynamic includes the changeover of FC control into the control of output current of FC, I_{fc}. That is,

$$I_{fc-ref} = \frac{P_{fc-ref}}{V_{fc}} \tag{3.4}$$

I_{fc-ref} is limited by the following two equations to ensure that the FC is operating within a safe operating area.

$$I_{fc-ref\,(\max)} = \frac{U_{\max}}{2K_r} q_{h2-in} \tag{3.5}$$

$$I_{fc-ref\,(\min)} = \frac{U_{\min}}{2K_r} q_{h2-in} \tag{3.6}$$

Where,

$$K_r = \frac{N_0}{4F}$$

Here the U_{max} and the U_{min} denotes the maximum and minimum fuel utilization respectively. N_0 means the number of fuel cells connected in series in the stack. F is the Faraday Constant and q_{h2-in} is the input flow rate of hydrogen. Now, a first order transfer function is used to model the dynamic.

$$I_{fc} = \frac{1}{1+T_e s} I_{fc-ref} \tag{3.7}$$

The dynamic of the fuel supply can be depicted by a first order transfer function.

$$q_{h2-in} = \frac{2K_r}{U_{opt}} \frac{1}{1+T_f s} I_{fc-ref} \tag{3.8}$$

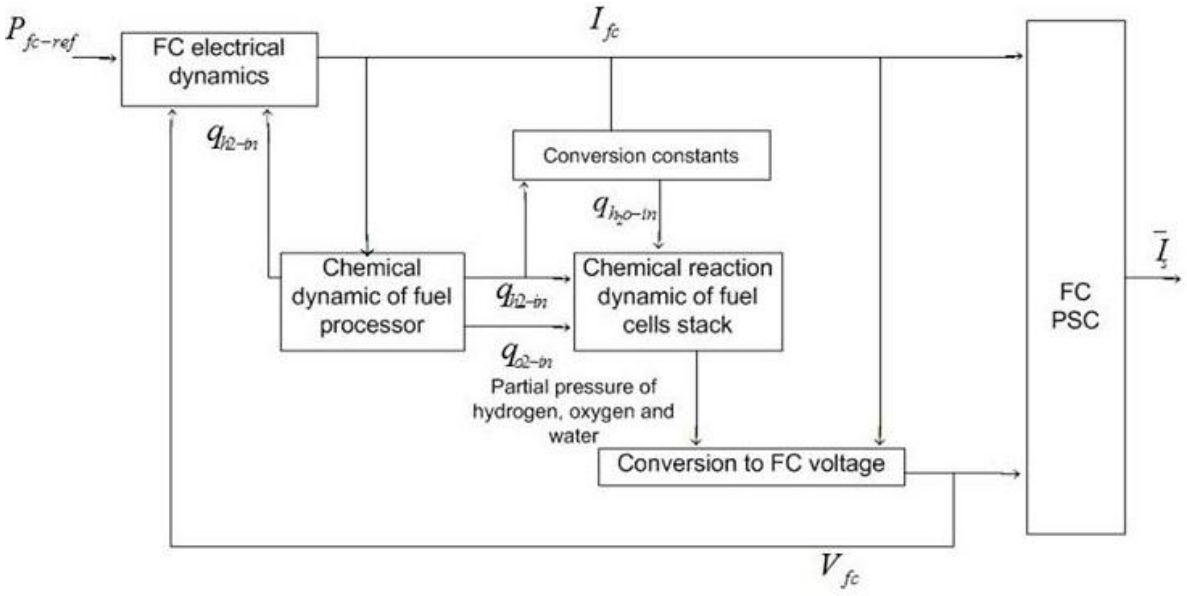

Fig.3.2 Functions block diagram of an SOFC

We have used U_{opt} to refer to the optimal utilization of fuel and T_f denotes the time constant of dynamic of fuel supply. From the equation of q_{h2-in} we can find q_{o2-in} through the following equation.

$$q_{o2-in} = \frac{1}{r_{ho}} q_{h2-in} \tag{3.9}$$

Where, r_{ho} represents the ratio of hydrogen and oxygen.

The partial pressures of hydrogen, oxygen and water is depicted by the following first order transfer functions:

$$P_{h2} = \frac{1}{K_{h2}} \frac{1}{1+T_{h2}s}(q_{h2-in} - 2K_r I_{fc})$$

$$P_{o2} = \frac{1}{K_{o2}} \frac{1}{1+T_{o2}s}(q_{o2-in} - K_r I_{fc})$$

$$P_{h2o} = \frac{1}{K_{h2o}} \frac{1}{1+T_{h20}s} 2K_r I_{fc} \tag{3.10}$$

K_{h2}, K_{o2} and K_{h2o} respectively refer the valve molar constant for hydrogen, oxygen and water. And T_{h2}, T_{o2} and T_{h20} are for time constants respectively.

The fuel cell stack voltage is constituted by the following equation:

$$V_{fc} = N_0[E_0 + \frac{RT}{2F}\ln(\frac{P_{h2} \times P^{.5}_{o2}}{P_{h2o}})] - rI_{fc} \tag{3.11}$$

Where,

E_0 = Ideal standard potential

R = Universal gas constant

T = Absolute temperature

r = Ohmic loss

The interface of SOFC power plant with the conventional power system consists of a dc-dc converter. This dc-dc converter is affiliated with a dc-dc controller. Fuel Cell current control is accomplished by the regulation of the dc-dc converter.

$$d_c = d_c + T_{dc}(s)(I_{fc-ref} - I_{fc}) \tag{3.12}$$

Where,

d_c = Duty cycle

$T_{dc}(s)$ = Transfer function of fuel cell current controller

From d-q coordinate of the generator we can obtain the ac voltage at the terminal voltage of dc-ac converter ,

$$V_c = mkV_{dc}(\cos\psi - j\sin\psi) = mkV_{dc}\angle\psi \tag{3.13}$$

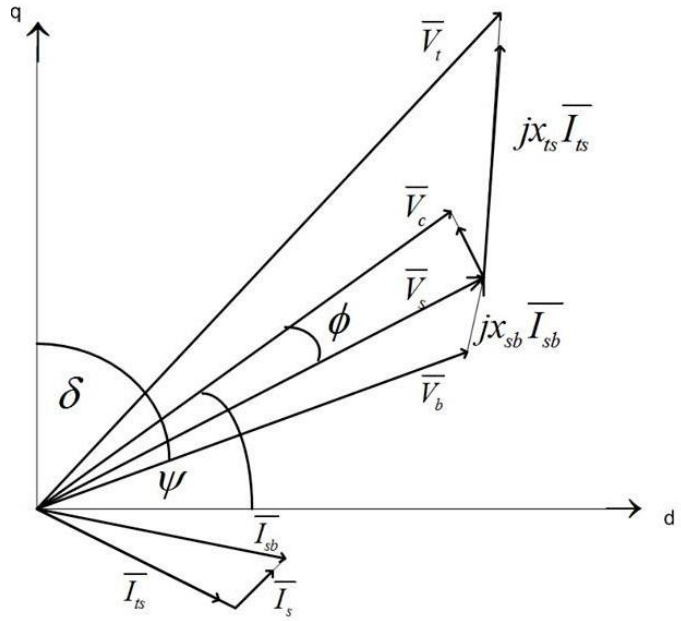

Fig.3.3 Phasor diagram of power system of Fig. 3.1

Where k is the converter ratio (typically k=3/4) in Fig. m and Q are respectively modulation ratio and phase of the width modulation (PWM) control algorithm of dc-ac converter. Active power received by the grid from the SOFC power plant is

$$V_{dc}I_{dc1} = i_{sd}v_{cd} + i_{sq}v_{cq} = i_{sd}mkV_{dc}\cos\psi + i_{sq}mkV_{dc}\sin\psi \tag{3.14}$$

where is i_{sd} and i_{sq} is the d and q component of $\overline{I}_s$, v_{cd} and v_{cq} that of $\overline{V}_c$,

respectively. Hence

$$I_{dc1} = i_{sd} mk \cos\psi + i_{sq} mk \sin\psi \tag{3.15}$$

The active power supply from the SOFC power plant is $P_{fc} = I_{fc} V_{fc} = I_{dc2} V_{dc}$ and $V_{dc} = \frac{V_{fc}}{(1-d_c)}$. Hence,

$$I_{dc2} = (1-d_c) I_{fc} \tag{3.16}$$

Dynamic equation of the dc – ac converter is

$$\dot{V}_{dc} = \frac{1}{C_{dc}} I_{dc} = \frac{1}{C_{dc}} (I_{dc2} - I_{dc1}) = \frac{1}{C_{dc}} [(1-d_c) I_{fc} - (i_{sd} mk \cos\psi + i_{sq} mk \sin\psi)] \tag{3.17}$$

3.3. Controller

To understanding the dc-ac conversion we have to apply PWM algorithm and V_{dc} must be constant anyway. In order to do that a dc voltage controller is introduced. Another thing modulation ratio which control the ac voltage V_s. therefore,

Dc voltage controller: $\phi = \phi_0 + T_{vdc}(s)(V_{dc} - V_{dc-ref})$ (3.18)

Ac voltage controller: $m = m_0 + T_{vac}(s)(V_s - V_{s-ref})$ (3.19)

where $T_{vdc}(s)$ and $T_{vac}(s)$ are the transfer function of dc voltage controller and ac voltage controller respectively.

The following equations can be obtained from Fig.1

$$\begin{aligned} \bar{V}_t &= j x_{ts} \bar{I}_{ts} + \bar{V}_s \\ \bar{V}_s &= -j(x_{cs} + x_{fs}) \bar{I}_s + \bar{V}_c = -j x_s I_s + \bar{V}_c \end{aligned} \tag{3.20}$$

$$\bar{V}_s + \bar{V}_b = jx_{sb}(\bar{I}_{ts} + \bar{I}_s)$$

The above equation give

$$-jx_s\bar{I}_s + \bar{V}_c - \bar{V}_b = jx_{sb}(\bar{I}_{ts} + \bar{I}_s) \quad (3.21)$$

$$\bar{V}_t = jx_{ts}\bar{I}_{ts} + jx_{sb}(\bar{I}_{ts} + \bar{I}_s) + \bar{V}_b \quad (3.22)$$

It can be obtained from (3.20) which come from Fig.1 is shown below in the d-q coordinate of the generator

$$x_{sb}i_{tsq} + (x_s + x_{sb})i_{sq} = -V_c\cos\psi + V_b\sin\delta \quad (3.23)$$

$$(x_q + x_{ts} + x_{sb})i_{tsq} + x_{sb}i_{sq} = V_b\sin\delta \quad (3.24)$$

$$x_{sb}i_{tsd} + (x_s + x_{sb})i_{sd} = V_c\sin\psi - V_b\cos\delta \quad (3.25)$$

$$(x'_d + x_{ts} + x_{sb})i_{tsd} + x_{sb}i_{sd} = E'_q - V_b\cos\delta \quad (3.26)$$

$$V_{sd} = x_s i_{sq} + kmV_{dc}\cos\psi \quad (3.27)$$

$$V_{sq} = -x_s i_{sd} + kmV_{dc}\sin\psi \quad (3.28)$$

The overall mathematical model of the power system is demonstrated which comprised of a SOFC Power plant and Single machine power plant grid connected to infinite bus. Actually the desegregation of a generator and SOFC is established. SOFC is considered to have more powerful and significant potential that's why we choose it beyond the other fuel cell.

Chapter 4
Results

4.1 Description

The test is done on a single machine infinite bus, shown in Fig.1. The system consists of a Generator, SOFC Connected to the grid, transmission line and infinite bus. The system is tested with different three different conditions,

1) With no disturbance and without using any controller
2) With disturbance and without using any controller
3) With disturbance and using three controller

In first condition we always get the system stable as all the curves are straight line. For the simplicity we ignore this part from our result portion. We added mechanical torque disturbance to the conventional generator and disturbance to Fuel cell output current. Disturbance added at time t=1sec and end at t=1.1 sec. As a consequence the system no more stable though we anticipated that system will stable after small oscillatory period. In order make unstable system stable three controllers are introduced. Using this controller the unstable system becomes moving to stable, after small oscillatory period the system again stable. For controller designing there are several controller parameters in our hand. Tuning these gain parameters the perfect matching is found. Controller is designed. Controller parameter gain are given below

$$K_{fc} = 5, \quad K_{fci} = 1.57, \quad K_{vaci} = 0.1$$
$$K_{vdc} = -0.8, \quad K_{vdci} = -9, \quad K_{dc} = 5$$

In our investigation voltage control scheme is used for converters though current control scheme can also be applied.

4.2 Simulation Results

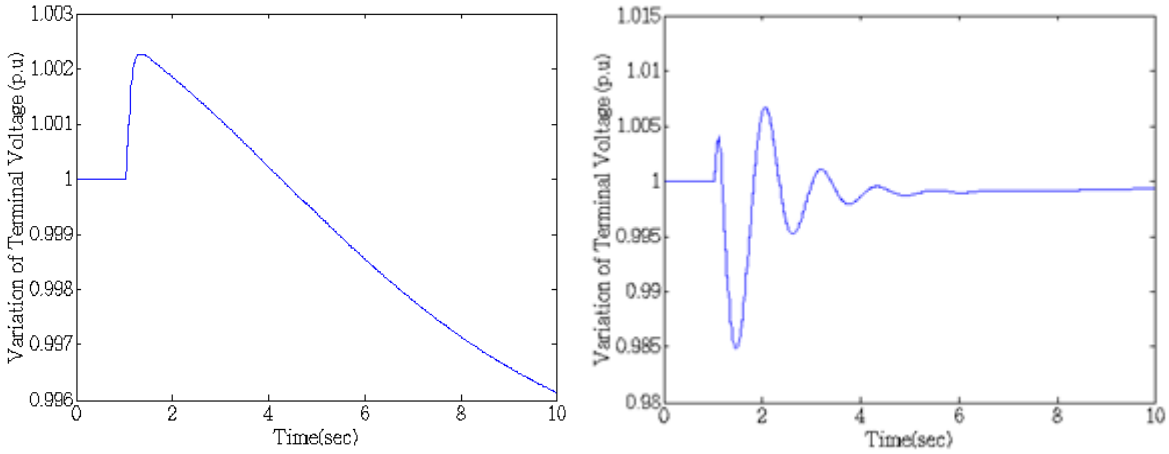

a b

Fig.4.1 Response of Terminal voltage for without controller (a) and with controller (b)

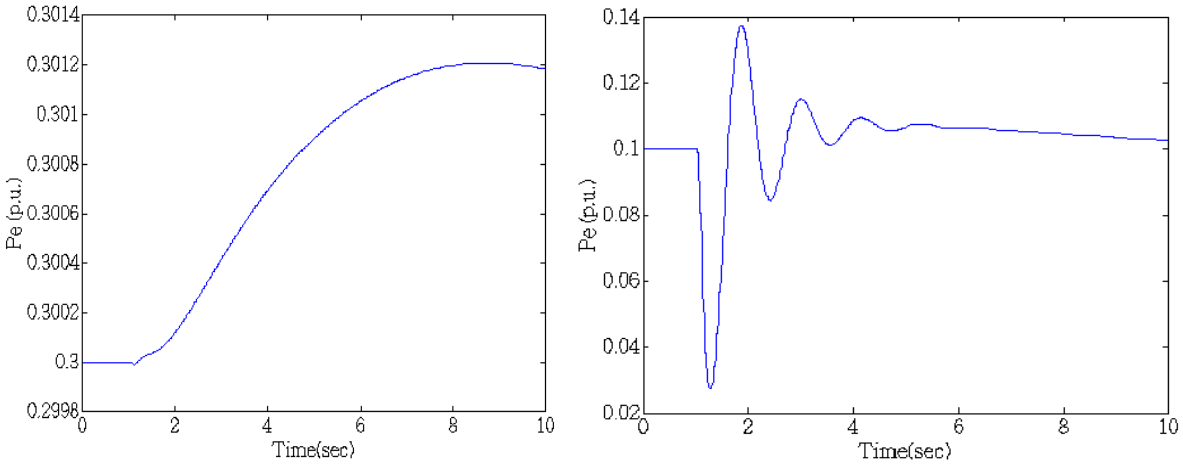

a b

Fig 4.2.Response of Total output power for without controller (a) and with controller(b)

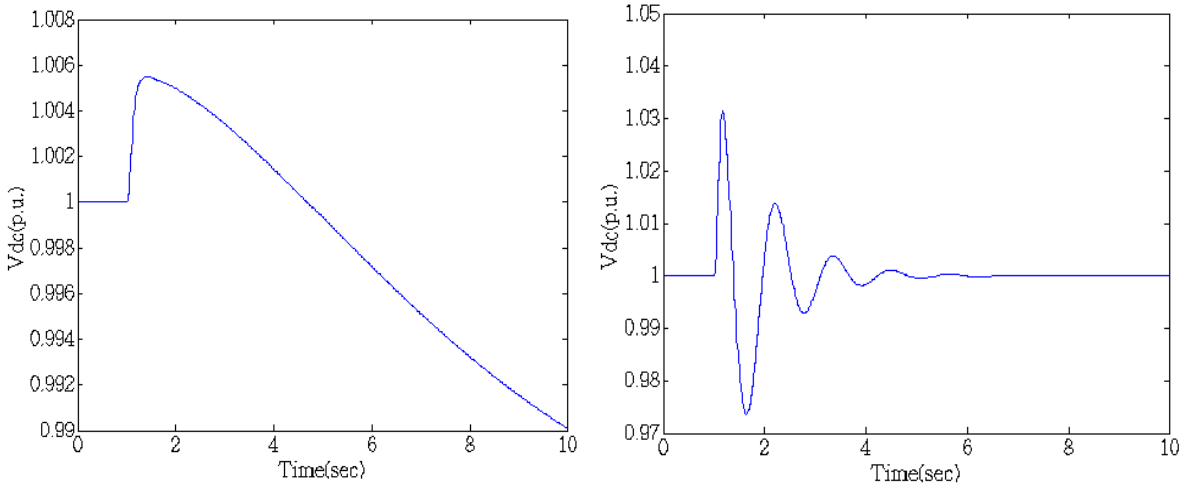

a b

Fig. 4.3. Response of Fuel cell dc output voltage for without controller (a) and with controller (b)

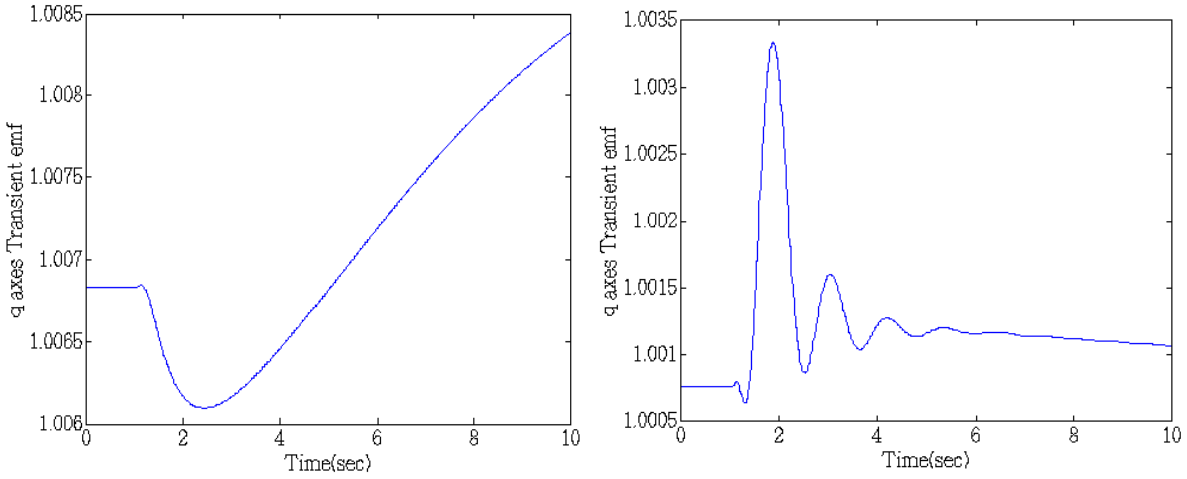

a b

Fig. 4.4 Response of Internal voltage for without controller (a) and with controller (b)

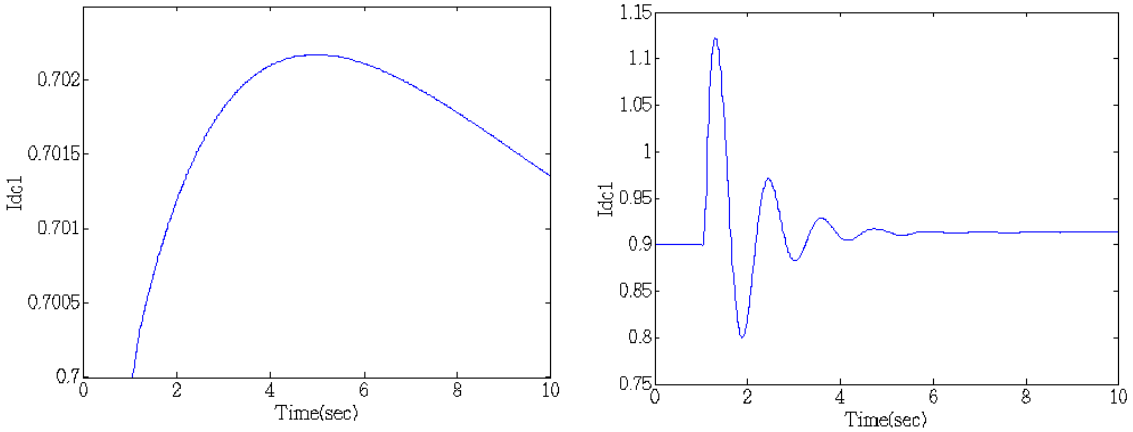

a b

Fig.4. 5. Response of Idc1 for without controller (a) and with controller (b)

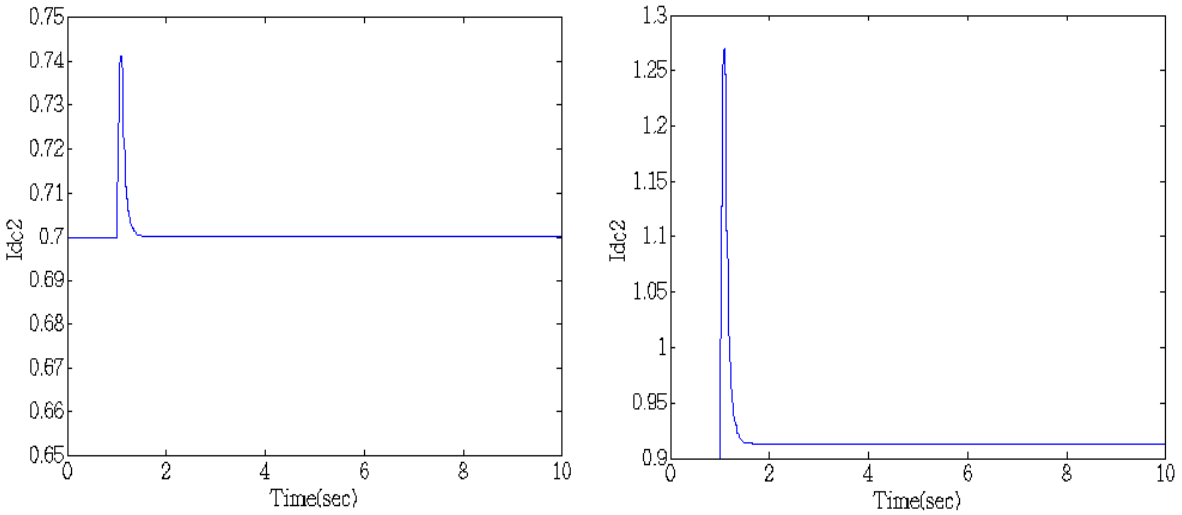

a b

Fig.4.6 . Response of Idc2 for without controller (a) and with controller (b)

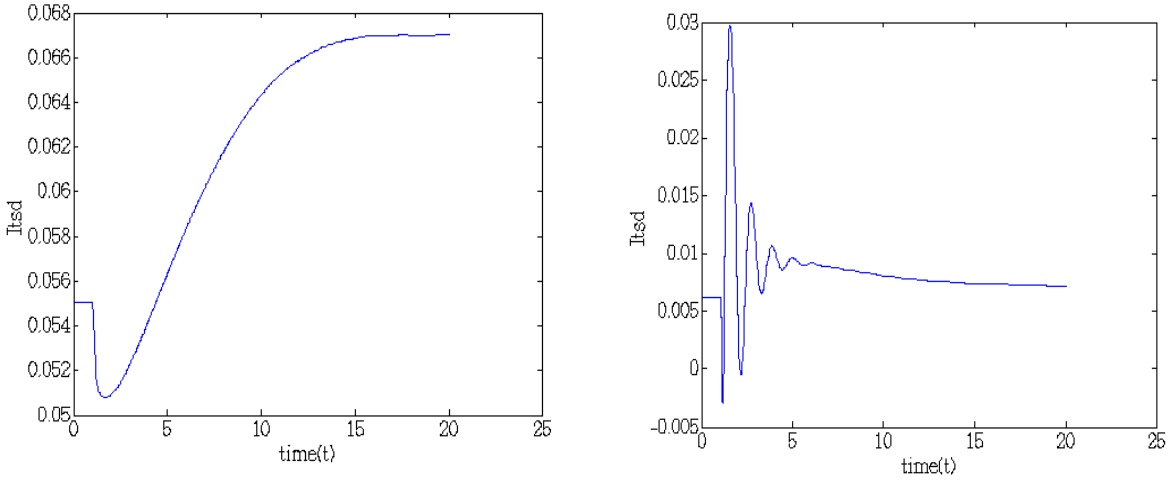

a b

Fig.4.7 . Response of Itsd for without controller (a) and with controller (b)

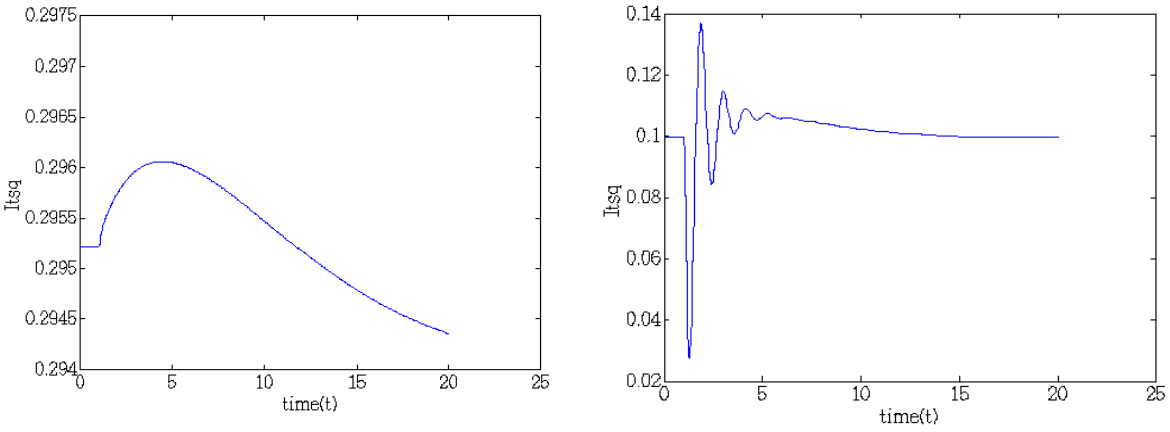

A b

Fig.4.8 Response of Itsq for without controller (a) and with controller (b)

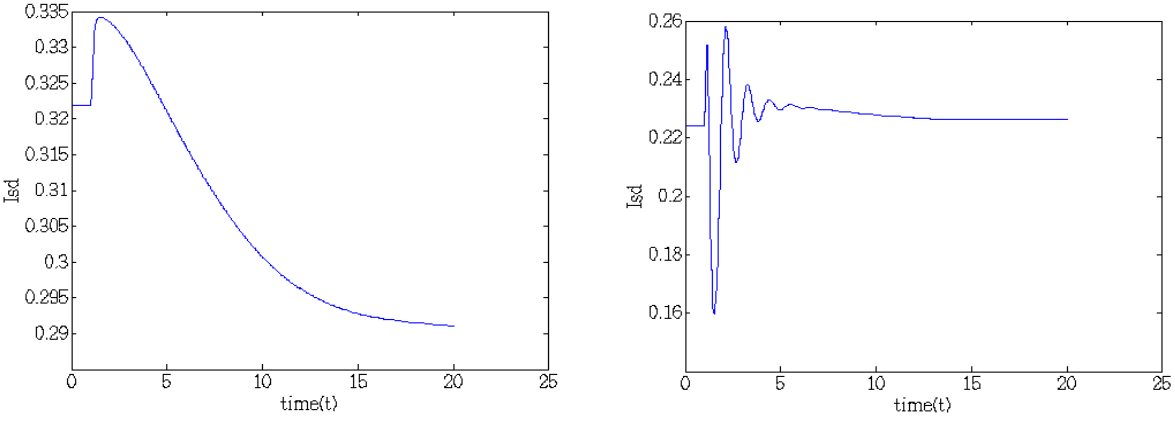

a b

Fig.4.9. Response of Isd for without controller (a) and with controller (b)

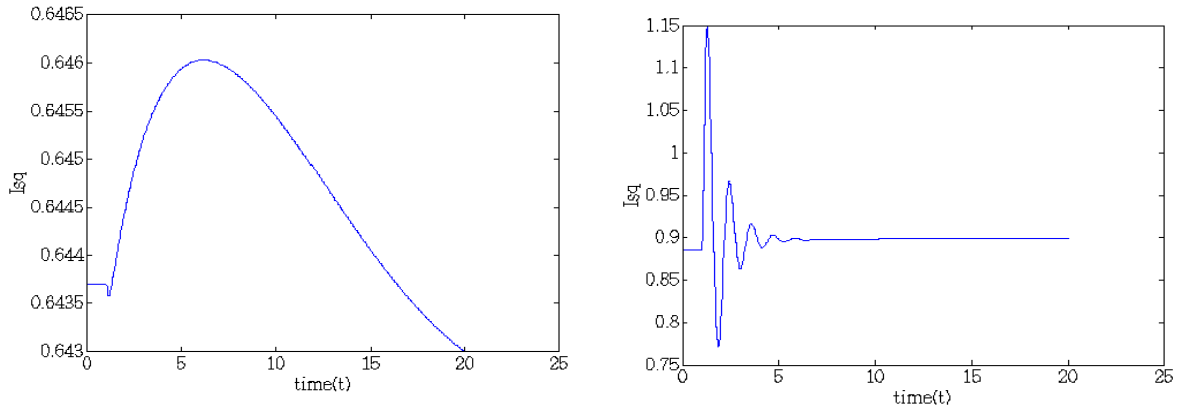

a b

Fig.4.10. Response of Isq for without controller (a) and with controller (b)

4.3 Conclusion

This paper presents the power system stability improvement by employing three FC controllers. In case of FC controller designing the controller gains are tuned manually. These controllers help the system regain stability after encountering mechanical torque disturbance.

The work demonstrated in this paper can lead to many promising thesis work. Our future ambition is to take this thesis work to the next level. First we wish to generate the linear model of our whole work. Then we wish to perform the simulation for different renewable sources, like Wind power plant, Solar Photovoltaic cell, Tidal power generation system and so on. We also possess a plan to perform the simulation for multi-machine system.

Appendix

Per unit values of the following parameters are used, including for the relevant dc system in the examples.

Parameters of the example single machine infinite-bus power system (machine damping coefficient includes the effect of the PSS. A relatively low gain automatic voltage regulator (AVR) is adopted.)

Transmission line:

$$x_{ts} = 0.3 p.u., x_{sb} = 0.3 p.u., x_s = 0.3 p.u., x_d = 1.3 p.u.,$$
$$x_q = 0.47 p.u., x'_d = 0.3 p.u., M = 7.4 p.u., D = 4 p.u., T'_{d0} = 5 s,$$
$$T_d = 0.1 s, K_A = 10 p.u.$$

Initial Load Condition:

$$V_{t0} = 1.0 p.u., V_{s0} = 1.0 p.u., V_{b0} = 1.0 p.u.$$

Converters (voltage control scheme)

$$m = m_0 + \left(K_{vac} + \frac{K_{vaci}}{s} \right)(V_{s-ref} - V_s)$$

$$\phi = \phi_0 + \left(K_{vdc} + \frac{K_{vdci}}{s} \right)(V_{dc-ref} - V_{dc})$$

$$C_{dc} = 1.0 p.u., V_{dc0} = 1.0 p.u., K_{vac} = -0.1, K_{vaci} = 0.1, K_{vdc} = -0.8,$$
$$K_{vdci} = -9, K_{dc} = 5$$

$$d_c = d_{c0} + \left(K_{fc} + \frac{K_{fci}}{s} \right)(I_{fc-ref} - I_{fc})$$

$$K_{fc} = 5, K_{fci} = 1.57$$

References

[1] Li, Y.H., Rajakaruna, S., Choi, S.S.: 'Control of a solid oxide fuel cell power plant in a grid-connected system', IEEE Trans. Energy Convers. , 2007, 22, (2), pp. 405 – 413

[2] W. D u, H.F. Wang, X.F. Zhang, L.Y. X iao: 'Effect of grid-connected solid oxide fuel cell power generation on power systems small-signal stability' , IET Renewable Power Generation , 2009

[3] Wenjuan DU, Haifeng Wang and Hui Cai: 'Modelling a grid -connecte d SOFC power plant into power systems for sm all-signal stabil ity analysis and cont rol', Int. Trans. Electr. Energ. Sys. 2013; 23 :330 –341

[4] Padulles, J., Ault, G.W., McDonald, J.R.: 'An integrated SOFC plant dynamic model for power systems simulation', J. Power Sources , 2000, 86, pp. 495 – 500

[5] Zhu, Y., Tomsovic, K.: 'Development of models for analyzing the load-following performance of microturbines and fuel cells', Electr. PowerSyst. Res., 2002, 62, pp. 1 – 11

[6] Georgakis, D., Papathanassiou, S., Manias, S.: 'Modelling and control of a small scale grid-connected PEM fuel cell system'. Proc. IEEE 36th Power Electronics Specialists Conf., 2005, pp. 1614 – 1620

[7] Sedghisigarchi, K., Feliachi, A.: 'Dynamic and transient analysis of power distribution systems with fuel cells – part I fuel-cell dynamic model', IEEE Trans. Energy Convers., 2004, 19, (2), pp. 423 – 428

[8] Sedghisigarchi, K., Feliachi, A.: 'Dynamic and transient analysis of power distribution systems with fuel cells – part II control and stability enhancement', IEEE Trans. Energy Convers., 2004, 19, (2), pp. 429 – 434

[9] Padiar, Power system dynamics-Stability and control